AIAA 2002-2466

Design and Validation of an Aeroacoustic Anechoic Test Facility

D. Jansson, J. Mathew, J. P. Hubner,
M. Sheplak, and L. Cattafesta

University of Florida
Gainesville, FL 32611

8th AIAA/CEAS Aeroacoustics Conference
June 17-19, 2002
Breckenridge, CO

Report Documentation Page

Form Approved
OMB No. 0704-0188

Public reporting burden for the collection of information is estimated to average 1 hour per response, including the time for reviewing instructions, searching existing data sources, gathering and maintaining the data needed, and completing and reviewing the collection of information. Send comments regarding this burden estimate or any other aspect of this collection of information, including suggestions for reducing this burden, to Washington Headquarters Services, Directorate for Information Operations and Reports, 1215 Jefferson Davis Highway, Suite 1204, Arlington VA 22202-4302. Respondents should be aware that notwithstanding any other provision of law, no person shall be subject to a penalty for failing to comply with a collection of information if it does not display a currently valid OMB control number.

1. REPORT DATE	2. REPORT TYPE	3. DATES COVERED
JUN 2002		**00-00-2002 to 00-00-2002**

4. TITLE AND SUBTITLE	
Design and Validation of an Aeroacoustic Anechoic Test Facility	5a. CONTRACT NUMBER
	5b. GRANT NUMBER
	5c. PROGRAM ELEMENT NUMBER
6. AUTHOR(S)	5d. PROJECT NUMBER
	5e. TASK NUMBER
	5f. WORK UNIT NUMBER
7. PERFORMING ORGANIZATION NAME(S) AND ADDRESS(ES) **University of Florida,Department of Electrical and Computer Engineering,Gainesville,FL,32611**	8. PERFORMING ORGANIZATION REPORT NUMBER
9. SPONSORING/MONITORING AGENCY NAME(S) AND ADDRESS(ES)	10. SPONSOR/MONITOR'S ACRONYM(S)
	11. SPONSOR/MONITOR'S REPORT NUMBER(S)

12. DISTRIBUTION/AVAILABILITY STATEMENT
Approved for public release; distribution unlimited

13. SUPPLEMENTARY NOTES
The original document contains color images.

14. ABSTRACT

15. SUBJECT TERMS

16. SECURITY CLASSIFICATION OF:			17. LIMITATION OF ABSTRACT	18. NUMBER OF PAGES	19a. NAME OF RESPONSIBLE PERSON
a. REPORT	b. ABSTRACT	c. THIS PAGE			
unclassified	**unclassified**	**unclassified**		**11**	

AIAA 2002-2466

Design and Validation of an Aeroacoustic Anechoic Test Facility

D. Jansson,[*] J. Mathew,[*] J. P. Hubner,[†] M. Sheplak,[§] and L. Cattafesta[‡]
Department of Mechanical and Aerospace Engineering
University of Florida, Gainesville, FL 32611-6250
(352) 846-3017, (352) 392-7303 (FAX)

Abstract

This paper discusses the design and initial validation of a newly constructed aeroacoustic anechoic test facility at the University of Florida. The facility will enable and assist research in the areas of aeroacoustics, structural acoustics, and industrial noise/vibration control. General facility features and characteristics are described and documented. Experimental results focus on the free-field characteristics of the chamber via the ISO 3745 standard and preliminary evaluations of the acoustic data quality for subsonic axisymmetric turbulent jet noise measurements. Initial free-field results comply with the tolerances set by the ISO standard except for a few bands close to the corner containing the chamber door. The preliminary jet noise measurements yield reasonable comparisons to the fine-scale turbulent jet noise similarity spectrum at 90^{o}. The results also reveal the need for acoustic treatment and vibration control of the chamber traverse and fan that supplies supplemental entrainment air.

Introduction

The University of Florida has recently completed the construction of an aeroacoustic anechoic chamber. The test facility, constructed by Eckel Industries, Inc. (http://www.eckelacoustic.com/), will enable research in the areas of aeroacoustics, structural acoustics, and industrial noise/vibration control. In addition, the facility will have a positive effect on research-related education at the University of Florida.

The immediate application of the facility is for scaled aeroacoustic testing. But before the facility can be used for research, careful experiments must be conducted to assess the acoustic and flow quality of the facility. Recently, Viswanathan addressed data quality issues with respect to jet noise.[1] He emphasized the importance of obtaining high quality jet noise data over a large frequency range for scaled model tests– typically from 200 Hz to 80 kHz.

The purpose of this paper is to report on the design, construction, and preliminary validation experiments of the facility. Two different approaches are taken for this purpose. The first method is concerned with the characteristics of the anechoic chamber and employs the ISO 3745 standard for free-field pressure measurements in an anechoic room.[2] This method is based on the well-established 6 dB decrease in sound pressure level (SPL) per doubling of distance from an omnidirectional source. However, this method is most suitable for audible frequencies, where the omnidirectional behavior of an acoustic source is readily achieved.

The second method is concerned with the data quality of aerodynamic noise from high-speed jets. This method exploits the universal fine-scale similarity noise spectrum associated with acoustic radiation at 90^{o} with respect to the incoming axis of a subsonic axisymmetric turbulent jet. Tam et al.[3,4] discuss the two self-similar components of turbulent mixing noise, namely the fine-scale spectrum alluded to above and the large-scale component that is dominant in the downstream quadrant close to the jet axis. By measuring the sound produced by a subsonic axisymmetric turbulent jet and comparing the results with the universal similarity spectrum, unwanted facility noise sources can be identified and reduced.

The paper is organized as follows. First, a general description of the facility design and characteristics is presented. Second, the chamber characterization study using the ISO 3745 standard is described. Third, the methodology and results of the jet noise experiments are discussed. The paper concludes with a summary and outlines directions for future work.

Facility Description

A top-view schematic of the facility is shown in Fig. 1. The University of Florida anechoic chamber is a room contained within a noise enclosure to minimize disturbances due to ambient noise and vibration. The inner dimensions from wedge tip to wedge tip of the anechoic chamber are 5.5 m long by 5.0 m wide by 2.3 m high. The wedges are constructed from fiberglass with cloth covers. The floor wedges are housed in carts with removable metal grates along the top to

[*]Graduate Research Assistant.
[†]Adjunct Assistant Professor, jph@aero.ufl.edu, Member AIAA.
[§]Assistant Professor, ms@aero.ufl.edu, Member AIAA.
[‡]Assistant Professor, catman@aero.ufl.edu. Senior Member AIAA.

allow walk-in access. With the floor wedge carts removed, the semi-anechoic height is 3.3 m. The wedges are designed to achieve a low-frequency cut-off of 100 Hz, which is the frequency at which the energy absorption coefficient drops below 99% or the pressure reflection coefficient exceeds 10%. The anechoic zone parallel to the floor at the designed cut-off frequency of 100 Hz is 3.8 m by 3.3 m. The 100 Hz cut-off was not chosen for scaled aeroacoustic simulation but to accommodate low-frequency requirements of industrial noise control applications.

For aeroacoustic applications, the chamber has intake and exhaust plenums on opposite ends. The wedges along the plenum walls have openings to allow entrained flow to pass through the chamber. Fig. 2 shows the adjacent intake plenum wall from inside the chamber. Each plenum is itself a noise enclosure with flow silencers to suppress ambient noise. The intake plenum also has adjustable flow restrictor panels to assist in the even distribution of the entrained flow. A variable-speed fan, downstream of the exhaust plenum silencers, assists in pulling the entrained flow through the chamber.

The intake plenum (Fig. 3) also houses the intermediate jet reservoir which is plumbed into a compressor facility outside the building through two control valves. The dual-screw compressor, rated for 28.3 m^3/s at 1.4 MPa can continuously feed a perfectly expanded 2.54 cm diameter Mach 2 jet. Two 17 m^3 storage tanks permit blowdown testing. Nozzle flow rates are set with PC-controllable pneumatic valves. Individual nozzles connect to the intake plenum reservoir via a 15 cm diameter supply pipe. The supply pipe diameter was chosen to minimize pressure losses and assure a large reservoir to nozzle exit area ratio. Within the pipe and upstream of the nozzle, flow conditioning honeycomb and screens are installed. The jet exhaust is captured by a 1 m x 1m acoustically-treated bell-mouth and a silencer that extends through the exhaust plenum.

Ambient chamber pressure, temperature, relative humidity, and nozzle stagnation pressure can be monitored during testing. Outfitted on the ceiling of the chamber is a fully-automated, five degree-of-freedom (three translations and two rotations) Brüel & Kjær (B&K) microphone positioning system (Fig. 4). It is operated via software with a multi-channel B&K PULSE data acquisition and analysis system that includes 1/8 in. and 1/4 in. pressure and free-field microphones, a sound intensity probe, and a MEMS acoustic array.[5] For high-bandwidth applications, a multi-channel VXI data measurement system is available (max. sampling rate = 196 kHz). Acoustic measurements can be complemented with corresponding fluid dynamic measurements using particle image velocimetry, laser Doppler velocimetry, flow visualization and hot-wire anemometry as well as corresponding structural dynamic measurements using accelerometers and a scanning laser vibrometer.

Chamber Characterization

Free-Field Characterization

The function of the anechoic chamber is to eliminate or minimize (within specified tolerances) the reflected or scattered sound energy from a source. If the reflected energy is small such that free-field conditions are approximated, the SPL from a point source emanating spherical waves should decrease in proportion to the radius squared (or 6 dB per distance doubling).

The ISO 3745 standard stipulates analyzer settings for anechoic and semi-anechoic chamber free-field characterization.[2] Between the center frequency of 125 Hz to 4000 Hz, octave frequency bands are selected. Above and below this range, 1/3rd -octave bands are employed. Both analyzers use constant percentage bandwidth (CPB) (i.e., the bandwidth is proportional to the center frequency of the band). The center frequencies are defined by ISO 266 as 80, 100, 125, 250, 500, 1000, 2000, 4000, 5000, 6300, 8000, and 12,500 Hz. Tolerances and quarter-wavelength distances (for T = 298 K) are listed in Table 1.

Table 1. SPL tolerances for free-field measurements.

Center Freq. (Hz)	CPB Analyzer	Tolerance (dB)	$\lambda/4^*$ (m)
100	1/3rd octave	+/- 1.5	0.87
125	octave	+/- 1.5	0.69
250	octave	+/- 1.5	0.35
500	octave	+/- 1.5	0.17
1000	octave	+/- 1.0	0.087
2000	octave	+/- 1.0	0.043
4000	octave	+/- 1.0	0.022
5000	1/3rd octave	+/- 1.0	0.017
6300	1/3rd octave	+/- 1.5	0.014
8000	1/3rd octave	+/- 1.5	0.011
10,000	1/3rd octave	+/- 1.5	0.0087
12,500	1/3rd octave	+/- 1.5	0.0069

*T = 298 K

Experimental Setup

Two different noise sources were used in the free-field characterization: (1) a B&K Omnisource speaker and (2) a JBL 2426H speaker mounted to a 0.53 m long, 19 mm diameter pipe (Fig. 5). Both received an amplified white-noise signal from a Crown K1 amplifier. The Omnisource speaker is omnidirectional between the frequency range of 80 to 6300 Hz (ISO 140 and ISO 3382 compliant). The loudspeaker radiates through a conical coupler through a circular orifice. The size of the orifice and the shape of the

Omnisource are designed to radiate evenly in all directions. It can be mounted horizontally or vertically on a standard tripod (the horizontal position was used in these experiments). The JBL speaker simulates an omnidirectional source for frequencies below 3 kHz. For higher frequencies, the radiator is no longer compact; therefore the radiation pattern is no longer omnidirectional. Hence, free-field measurements at high frequencies using the JBL speaker were conducted along a path directly opposite of the source. The practical low-end frequency for the JBL-tube design was ~1000 Hz due to poor driver efficiency at low frequencies.

A 1/8 in. condenser microphone was used to measure the free-field SPL (B&K Type 4138). The driver signal was amplified to produce a SPL of approximately 100 dB (re 20 μPa) at 4000 Hz at a distance of a quarter wavelength from the source. The microphone axis was positioned to point towards the exit plane of the noise source. The microphone was then traversed in the horizontal plane of the noise source (1.16 m above the floor grating) along radial lines extending from the noise source and towards the chamber walls. The noise source exit plane was placed in the center of the chamber. Eight rays were traversed: four to the center of each wall designated N(orth), E, S, and W, and four to the corner of two adjacent walls designated NE, SE, SW, and NW. For this designation, the bell-mouth is located on the N wall (see Fig. 1). The starting location for the SPL measurements was 0.197 m. The microphone was then traverse in steps ranging from 0.9 to 0.14 m for a total of 20 to 23 measurement positions depending on the path.

For theoretical free-field comparisons, the starting measurement location was chosen to be at least a quarter-wavelength from the source. The position of the noise source was set such that it faced the wall/corner in which the microphone was traversing towards. Data was collected and analyzed using the B&K PULSE system. Acquisition times were 15 s and data was linearly averaged with equal weighting. Octave and third–octave CPB analyzers were used to generate the SPL spectra (see Table 1).

Results

Fig. 6-8 are representative plots of the difference between the measured and theoretical free-field SPL (labeled N, NE, and E, respectively). Each figure is a stacked series of plots corresponding to the center frequency band when using the Omnisource speaker. The vertical axis corresponds to a +/- 2.5 dB range. The square symbols represent the measured difference and are bounded by the corresponding free-field tolerance for each frequency band. For the data shown, nearly all of the measurements are within tolerance. However, in the NE direction, the 250, 4000, and 5000 Hz fall out of tolerance near the double doors. Also, the 250 Hz in the N direction and the other three diagonal directions slightly exceed the tolerance as one approaches within one wavelength of the wall. All other center bands and directions fall into tolerance including the higher frequencies tested with the JBL-tube configuration (8000, 10,000, and 12,500 Hz).

Possible causes for the tolerance violations near the corners at 250 Hz and near the NE corner at 4000 and 5000 are exposed metallic components, such as door handles, door hinge posts, the traversing system structure, etc. These items will be covered/wrapped to minimize sound reflections in the next set of characterization tests. Additionally, trajectories starting from the chamber center and extending towards the ceiling and floor corners will be conducted. This is of interest due to possible reflections emanating from the traversing system structure that is mounted to the ceiling. Cross-spectra (not shown) between a microphone and an accelerometer fixed to the structural members of the traverse clearly indicated coherent power peaks at approximately 2.0 kHz and 3.2 Hz. Further discussion of this response will be presented in the next section on jet noise measurements.

Jet Noise Characterization

Experimental Setup

Four B&K 1/4 in. Type 4939-A011 free-field microphones with B&K Type 2633 preamplifiers and B&K Type 2804 power supplies were used for measuring the jet noise spectra. The microphones possessed a frequency range of 4 Hz to 100 kHz. The dynamic range of the microphones was 28 to 167 dB. Prior to taking jet noise measurements, the microphones were calibrated using a B&K Type 4228 pistonphone that provided a nominal amplitude of 124.7 dB at a frequency of 251.2 Hz.

Both third-octave band and narrow band noise spectra of the jet were measured. Data acquisition was carried out using an HP E1433A VXI system. An ANSI S1.11-1986 compliant LabVIEW Third Octave Analyzer was used to measure the third-octave band jet noise spectra. The frequency span for the third octave measurement was set at 76.8 kHz, which permitted third-octave bands up to 63 kHz. Jet noise data from the microphones were acquired and processed in a real-time continuous mode using linear averaging of 8192 samples in each block. Approximately 90 averages were performed before filling the data acquisition system buffer. These acquisition and processing parameters resulted in statistically converged spectra.

The schematic of the experimental test setup is shown in Fig. 9 and 10. The four microphones were aligned at azimuthal angles of 90°, 110°, 130° and 140° with respect to the incoming axis of the jet. The radial distances from the nozzle exit plane to the microphones are indicated in Fig. 9. The microphones were attached to the traverse rail, which runs along the West wall ceiling of the anechoic chamber. The microphones were pointed towards the exit plane of the nozzle using a laser pointer. Correct alignment of the microphones in this manner is consistent with free field measurements from a point source located at the nozzle exit plane. In order to minimize the effects of scattering, the protective grid of the microphones were removed prior to any measurements.

Acoustic noise measurements were performed for seven different Mach numbers ranging from approximately 0.3 to 0.9. An axisymmetric jet nozzle of inner diameter of 35.6 mm and wall thickness of 3.2 mm was used. The stagnation pressure inside the jet reservoir and the static pressure inside the anechoic chamber using a static pressure ring were measured to compute the nozzle pressure ratio and jet exit Mach number. The actual Mach number was subsequently verified by mounting a pitot probe at the exit of the nozzle, and measuring the pressure ratio between nozzle exit stagnation pressure and the chamber static pressure. The jet pressure ratio was maintained via software control of a valve using LabVIEW.

Results

Various configurations were tested in an effort to determine the influence of the following: floor grating and wedge configurations, ambient noise, traverse mechanism reflections, entrainment fan noise contamination, and compressor noise and vibration. This section summarizes the most pertinent results.

The chamber contains removable floor wedges to simulate a semi-anechoic test environment. The floor wedges are installed in carts with casters. Each cart has a removable floor grating. Not surprisingly, the optimum configuration required removal of the wedges from the carts, thereby maximizing the distance from the jet axis to the wedge tips on the chamber floor (0.44 m.). However, a row of carts on the outer rim of the chamber were subsequently reinstalled to permit access to the chamber and the microphones. Experiments showed that the peripheral row of carts did not affect the results.

Fig. 11 contains the measured noise floor of the 1/4 in. microphone at 90° with respect to the jet axis and the third-octave band B&K noise-floor specification at 1 kHz. The measured noise floor is within 1 dB of the B&K specification. This indicates that sufficient suppression of ambient noise has been achieved for aeroacoustic applications. The noise floor is below 36 dB from 100 Hz to 63 kHz. The data at the lowest Mach number = 0.3 are clearly limited at the lowest and highest frequencies by the noise floor of the microphone measurement.

Fig. 11 also shows the results obtained for the microphone located at 90° as a function of the exit jet Mach number. The nozzle pressure ratio was varied to achieve Mach numbers from 0.3 to 0.9 in steps of 0.1. Superimposed on the plot is the fine-scale noise similarity spectrum, $G\left(f/f_p\right)$, presented in Tam and Zaman,[4] corresponding to an observed peak frequency $f_p \approx$ 3.2 kHz using a narrow-band spectrum analyzer. As previously noted, this also corresponds to a resonant frequency of the traverse support rails. The similarity spectrum was integrated over third-octave bands to compare with the experimental data.

Several conclusions can be drawn from Fig. 11. First, the data at the lower Mach numbers are clearly corrupted, particularly at high frequency. The low Mach number data reveal high frequency noise contamination, the source of which has yet to be identified and eliminated. Second, the data in the mid-frequency (2-10 kHz) range are characterized by amplitude ripple. Various contaminating noise sources were systematically identified and eliminated, leading to Fig. 11. However, acoustic absorbing material was not yet available at the time of these tests to wrap the traverse mechanism (see Fig. 4), which served as the mount for the microphone holders. We suspect that reflections from the traverse rails are the primary cause of the observed ripple in the data.

Despite these issues, the data exhibit some expected trends. The data follow the fine-scale self-similar spectral shape. It should be cautioned that these free-field microphone data have not been corrected for atmospheric attenuation, which is significant at high frequency. Preliminary estimates of corrections based on the work of Shields and Bass[6] indicates adjustments ranging from ~1 dB near 20 kHz to ~7 dB at 63 kHz.

Fig. 12 compares the results between the 90° and 140° microphones for M=0.9. Superimposed on the figure are the large-scale (F) and fine-scale (G) noise similarity spectra. As expected, the results show that the 140° location in the downstream quadrant is significantly influenced by the large-scale noise, while the opposite is true for the 90° data.

Fig. 13 shows the effects of the entrainment fan operating at maximum volume flow capacity. By comparing directly with Fig. 11, the noise introduced by the fan is significant at both very low and very high frequencies, as well as approximately 3.2 kHz, corresponding to a resonance frequency of a traverse support beam. This demonstrates the need for better acoustic/vibration control for the fan and traverse.

A common approach to minimizing contamination due to flow noise is to run in a blowdown mode, in which the storage tanks are filled and the compressor is either isolated or (as in the case here) shut off completely. Fig. 14 shows a comparison between blowdown (compressor off) and continuous operation (compressor on) modes. The two test conditions are approximately the same (M=0.7±0.01, 90^o), although the blowdown run introduces some very low frequency (< 100 Hz) variations that are not visible in the plot. The data are nearly identical. The operation of the compressor may have little effect on the acoustic data due to the large distance between the compressor, the large pipe diameters, and the jet flow conditioning. In any case, this result suggests that the compressor need not be turned off or isolated during testing.

Conclusions and Future Work

This paper discusses the design and initial validation of a newly-constructed aeroacoustic anechoic test facility at the University of Florida. The facility was constructed and installed by Eckel. The anechoic chamber is a room contained within a noise enclosure to minimize disturbances due to ambient noise and vibration. The inner dimensions from wedge tip to wedge tip of the anechoic chamber are 5.5 m long by 5.0 m wide by 2.3 m high. With the floor wedge carts removed, the semi-anechoic height is 3.3 m. The low-frequency cut-off is 100 Hz. The facility enables research and teaching in the areas of aeroacoustics, structural acoustics, and industrial noise/vibration control provided the facility performance is validated.

Experimental results thus far have focused on the free-field characteristics of the chamber via the ISO 3745 standard and preliminary evaluations of the acoustic data quality for cold subsonic axisymmetric turbulent jet noise measurements. The free-field results comply with the tolerances set by the ISO 3745 standard, except for a few bands close to the corner containing the chamber door. The deviations are likely due to reflections from door components.

Low noise-floor measurements have been obtained that are less that 36 dB from 100 Hz to 63 kHz and are within 1 dB of the nominal B&K 1/4 in. microphone specification at 1 kHz, indicating sufficient isolation from ambient disturbances for aeroacoustic applications. The initial jet noise measurements yield reasonable comparisons to the fine-scale turbulent jet noise similarity spectrum at 90^o. However, the third-octave band data are characterized by some ripple in the 2-10 kHz range, presumably due to the large, acoustically-untreated traverse in the chamber. Additional sound field surveys along radial lines emanating from the jet location to the locations of the microphones will be conducted to quantify this phenomena. Efforts are underway to reduce the resonant scattering from the traverse rails.

Low Mach number jet noise data reveal the presence of some high frequency noise contamination that is masked at higher jet Mach numbers. Additional narrow-band auto- and cross-spectra will be obtained to determine the contamination source.

The supplemental entrainment exhaust fan was observed to inject significant noise contamination. This is presumably due to insufficient isolation between the fan and the chamber and will require further study. Smoke-flow visualization studies are currently being conducted to assess the impact of the entrainment fan on the jet flowfield, in addition to the acoustics. Very preliminary results indicate that the porous wedges in the front and real walls of the chamber, which are coupled to external air via silencers, are successful at eliminating problematic recirculating flow regions in the chamber.

Acknowledgements

The authors would like to acknowledge the financial support of the Air Force Office of Scientific Research through the DURIP program, monitored by Steve Walker and John Schmisseur. The authors would also like to thank Jack Seiner and K. Viswanathan for insight and advice.

References

1. Viswanathan, K., “Quality of Jet Noise Data: Issues, Implications, and Needs,” AIAA Paper 2002-0365, Jan. 2002.
2. “Acoustics — Determination of Sound Power Levels of Noise Sources — Precision Methods for Anechoic and semi-anechoic Rooms,” *International Standard ISO 3745*, 1977.
3. Tam, C. K. W., Golebiowski, M., and Seiner, J. M., “On the Two Components of Turbulent Mixing Noise from Supersonic Jets,” AIAA Paper 96-1716, May 1996.
4. Tam, C. K. W. and Zaman, K. B. M. Q., “Subsonic Jet Noise from Nonaxisymmetric and Tabbed Nozzles,” AIAA Journal, Vol. 38, No. 4, 2000, pp. 592 – 599.
5. Arnold, D. P., Nishida, T., Cattafesta, L. N., and Sheplak, M., “MEMS-Based Acoustic Array Technology,” AIAA Paper 2002-0253, January 2002.
6. Shields, F. D. and Bass, H. E., “Atmospheric Absorption of High Frequency Noise and Application to Fractional-Octave Bands,” NASA CR-2760, June 1977.

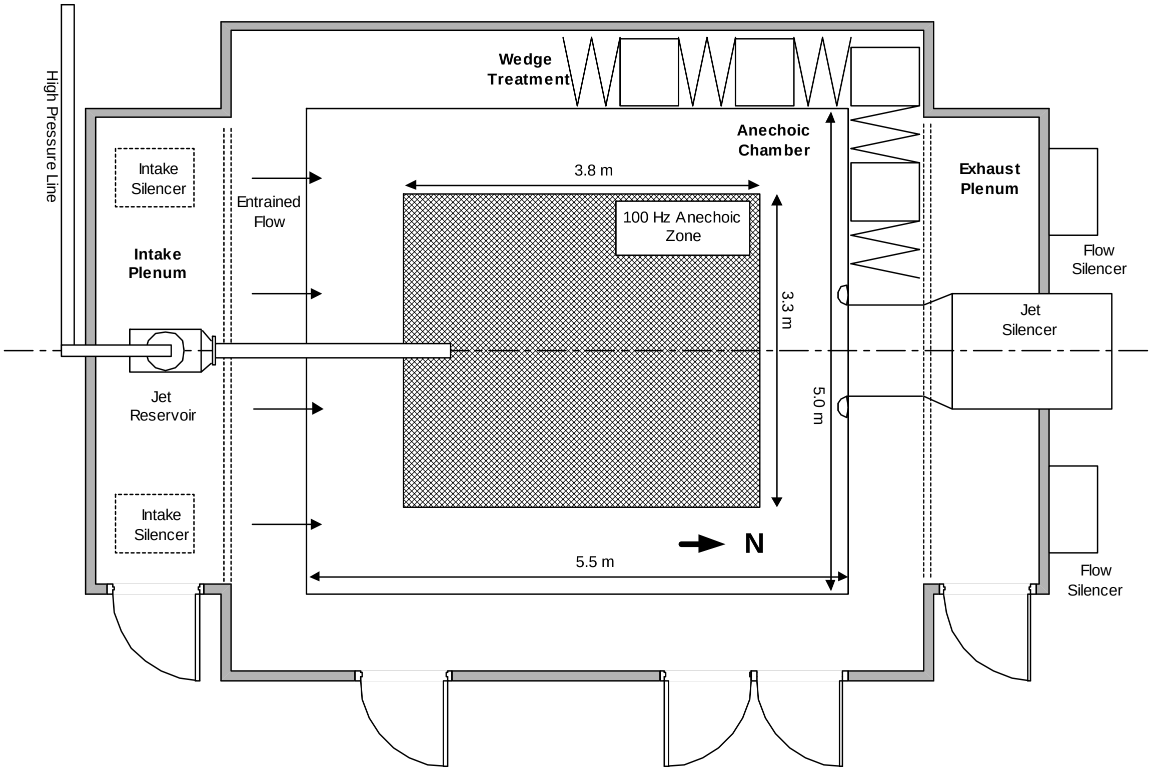

Fig. 1: Top view schematic of the anechoic chamber. The North wall corresponds to the jet exhaust.

Fig. 2: Image of the partial wedge openings along the intake plenum wall as viewed from inside the anechoic chamber.

Fig. 3: Image of the jet reservoir inside the intake plenum shown without flow restrictors.

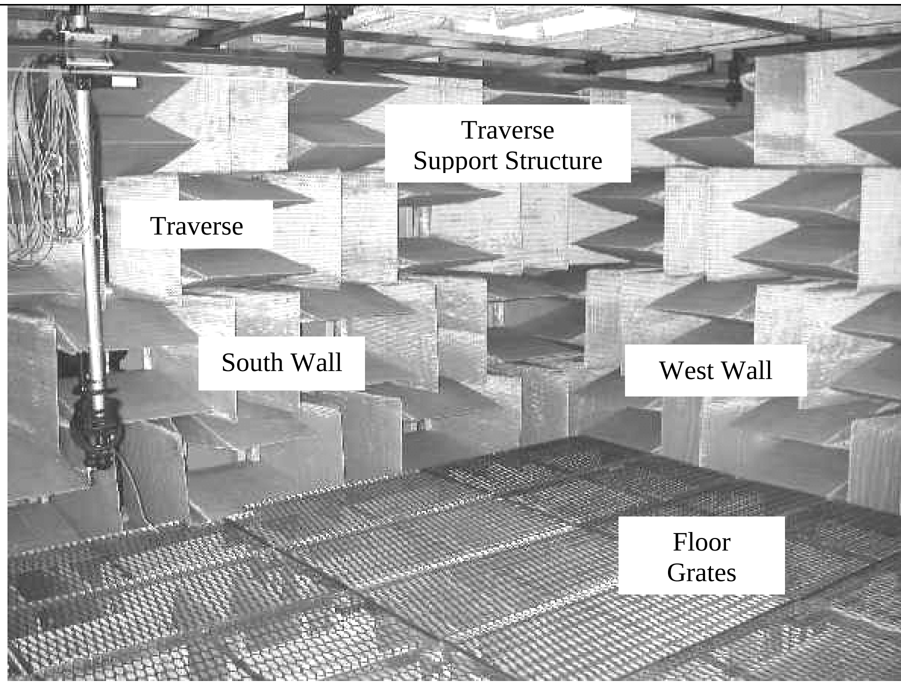

Fig. 4: Image of the interior of the anechoic chamber with floor grates and traverse mechanism.

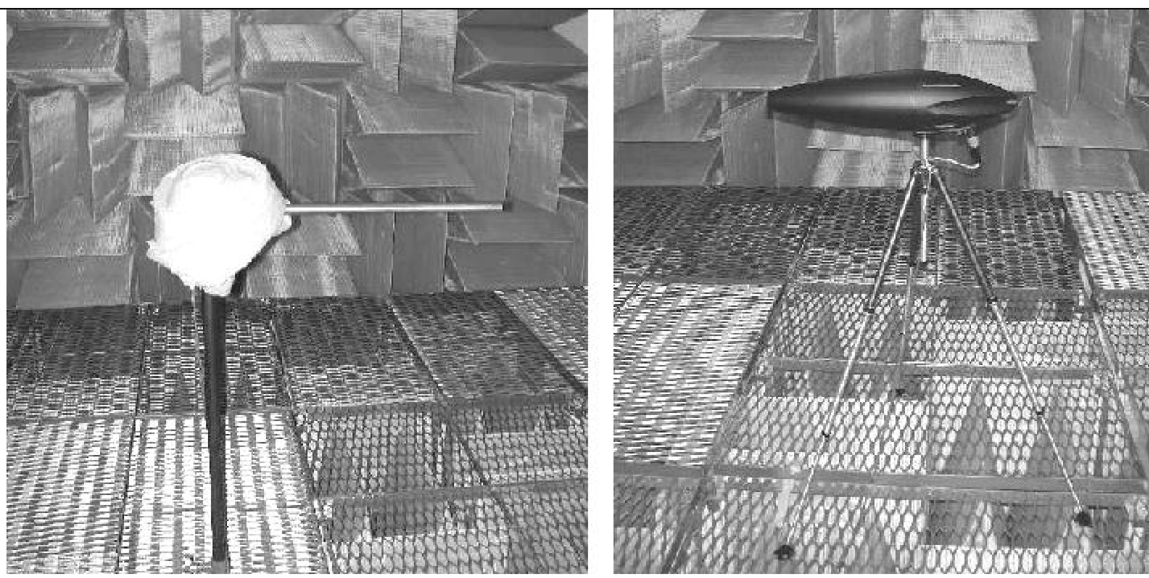

Fig. 5: The JBL speaker with the tube (left) and the Omnisource speaker (right).

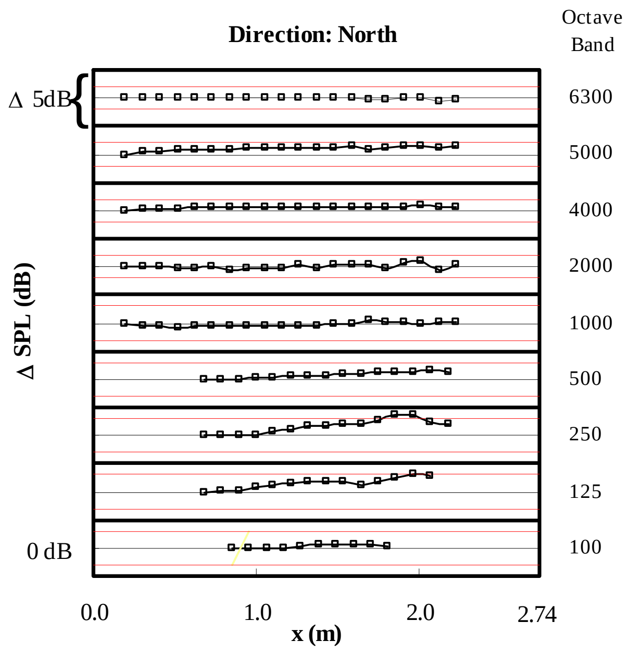

Fig. 6: Deviation of pressure measurements from free field from chamber center towards bell-mouth.

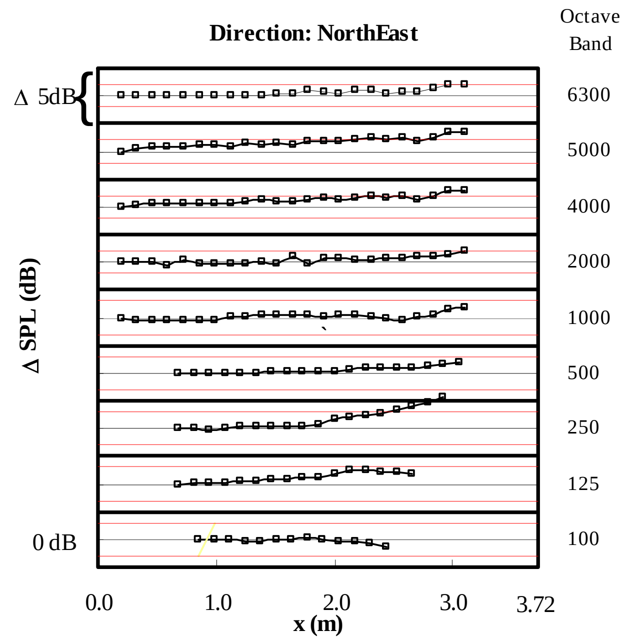

Fig. 7: Deviation of pressure measurements from free field from chamber center towards Northeast corner of room with double door.

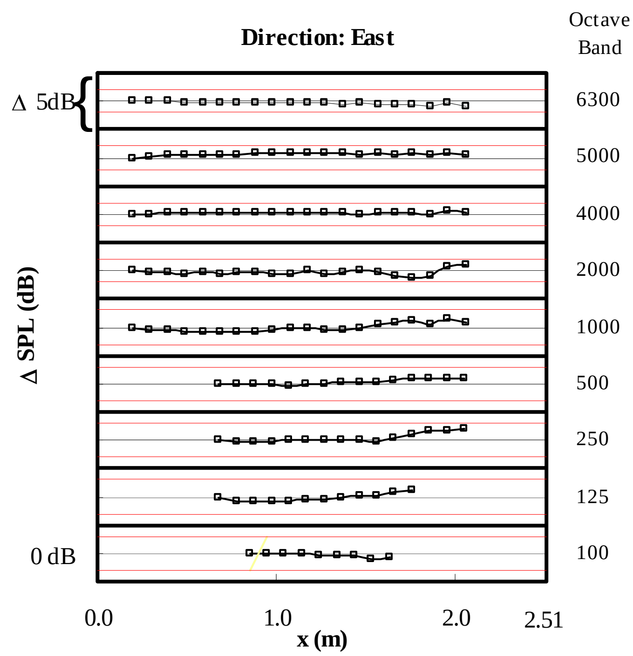

Fig. 8: Deviation of pressure measurements from free field from chamber center towards East wall.

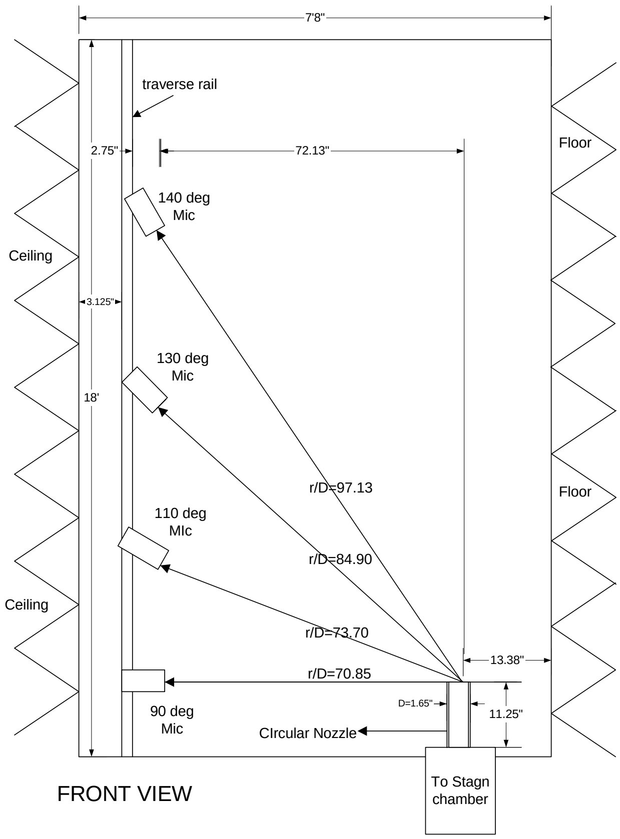

Fig. 9: Side view schematic of the jet noise measurements.

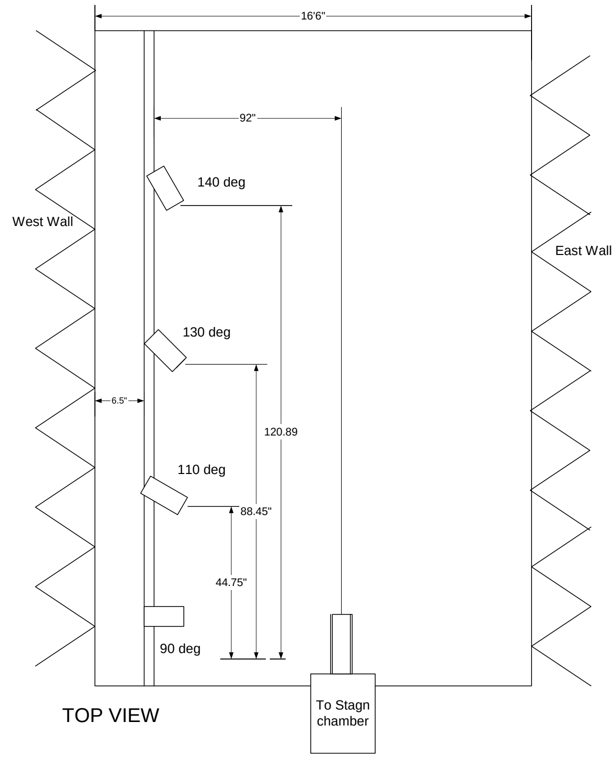

Fig. 10: Top view schematic of the jet noise measurements.

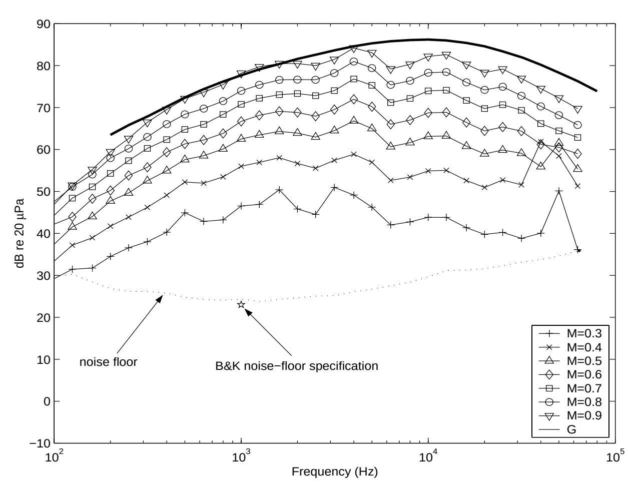

Fig. 11: Cold jet noise data measured at 90° to the jet axis at 83.5 jet diameters for various jet Mach numbers. Exhaust fan is off.

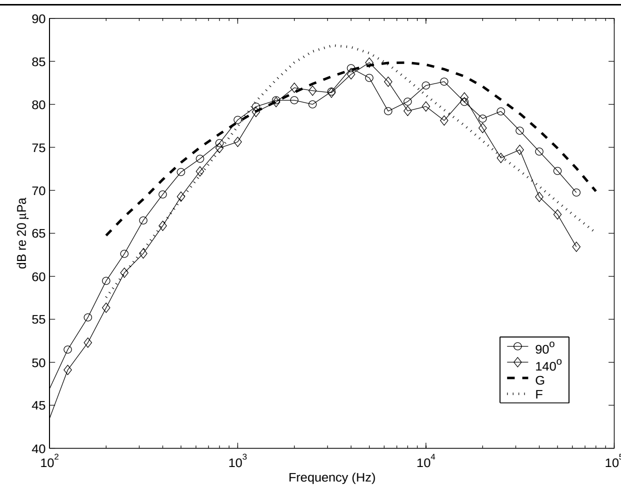

Fig. 12: Cold jet noise data measured at 90° and 140° to the jet axis at 83.5 and 114.5 jet diameters, respectively, at M=0.9. Exhaust fan is off. F and G are the large- and fine-scale similarity third-octave band spectra.

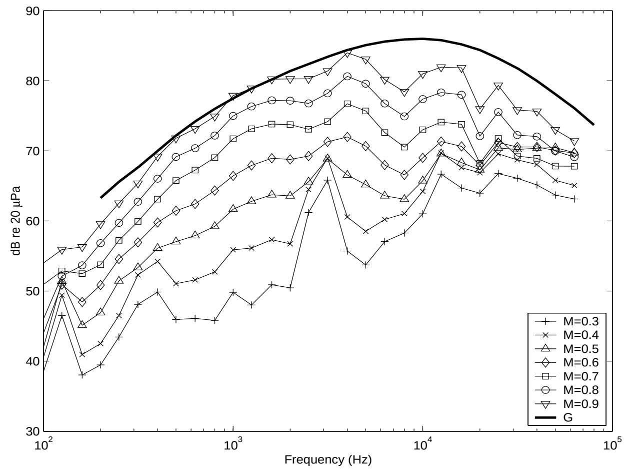

Fig. 13: Cold jet noise data measured at 90° to the jet axis at 83.5 jet diameters for various jet Mach numbers. Exhaust fan is operating at max speed (~6000 CFM).

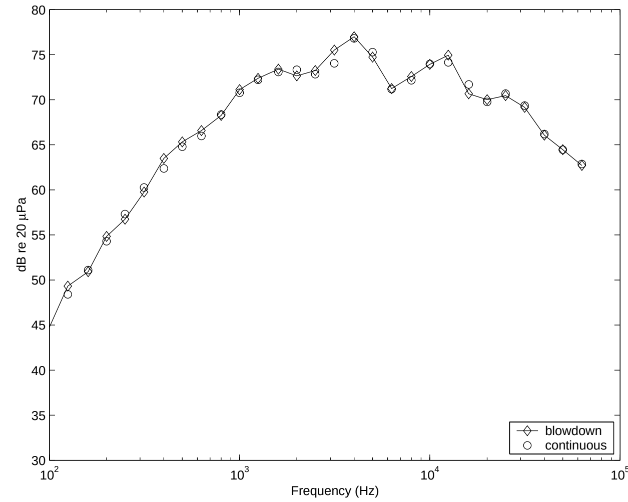

Fig. 14: Comparison between blowdown (compressor off) and continuous (compressor on) operating conditions for approximately identical flow conditions (M=0.7±0.01).